Journal of Environmental Chemical Engineering 8 (2020) 103654

Contents lists available at ScienceDirect

Journal of Environmental Chemical Engineering

journal homepage: www.elsevier.com/locate/jece

f-MWCNTs/AgNPs-coated superhydrophobic PVDF nanofibre membrane for organic, colloidal, and biofouling mitigation in direct contact membrane distillation

Lebea N. Nthunya[a,b,c,*], Leonardo Gutierrez[b,d], Edward N. Nxumalo[c], Arne R. Verliefde[b], Sabelo D. Mhlanga[e], Maurice S. Onyango[a]

[a] Department of Chemical, Metallurgical and Material Engineering, Tshwane University of Technology, Private Bag x680, Pretoria, 0001, South Africa
[b] Particle and Interfacial Technology Group, Department of Applied Analytical and Physical Chemistry, Ghent University, Coupure Links 653, 9000, Ghent, Belgium
[c] Nanotechnology and Water Sustainability Research Unit, College of Science, Engineering and Technology, University of South Africa, FL, 1709, Johannesburg, South Africa
[d] Facultad del Mar y Medio Ambiente, Universidad del Pacifico, Guayaquil, Ecuador
[e] DST/MINTEK Nanotechnology Innovation Centre, Strijdom Park, Randburg, 2125, Johannesburg, South Africa

ARTICLE INFO

Keywords:
Direct contact membrane distillation
Membrane fouling
Modified-PVDF nanofibre membrane
Resistance to flux and salt rejection decline

ABSTRACT

While membrane distillation (MD) is considered a promising cost-effective and efficient desalination process, it remains severely affected by membrane fouling that compromises the quantity and quality of water recovered. In this study, superhydrophobic PVDF membranes modified with organically-functionalised silica (f-SiO_2) nanoparticles (NPs) were synthesized. Silica nanoparticles (SiO_2NPs) were functionalised with three different silane reagents, namely: octadecyltrimethoxysilane (OTMS), N-octadecyltrichlorosilane (ODTS), and chlorodimethyl-octadecyl silane (Cl-DMOS), and finally embedded on polyvinylidene fluoride (PVDF) nanofibre membranes using an in-situ electrospinning technique. The resulting superhydrophobic membranes were coated with a thin layer containing carboxylated multiwalled carbon nanotubes (f-MWCNTs) and silver nanoparticles (AgNPs) to reduce membrane fouling. Fouling tests were conducted using sodium alginate, colloidal silica, and thermophilic bacteria effluent as model organic, inorganic, and bio-foulants, respectively, in direct contact membrane distillation (DCMD). The uncoated membranes were characterized by flux decays ranging from 30 to 90% and salt rejection decays of 1.4–6.1 %. Membrane coating reduced the flux and salt rejection decays to 10–24 % and 0.07–0.75 %, respectively. The hydrophilic coating layer of the nanofibre membrane induced a decrease in the initial water flux (i.e., from 36-42 LMH to 16–17 LMH). However, this coating layer also proved to be efficient in maintaining high salt rejection and resistance to flux decline. This approach is a suitable one-step solution for fouling mitigation in DCMD

1. Introduction

Scarcity and pollution of water are the main threats that affect all countries [1–4]. However, the desalination of saline water would offer a suitable alternative for tackling worldwide freshwater stress [5,6]. Since its initial development, membrane technology has evolved as a key approach to address the challenges associated with water scarcity and quality. Briefly, membrane processes used in water desalination include reverse osmosis (RO), forward osmosis (FO), and nanofiltration (NF) [7]. These processes are high pressure-driven, energy-demanding and therefore costly [8]. As such, membrane distillation (MD) has emerged as a promising cost effective desalination technology since it operates at lower pressures (i.e., lower energy) compared to RO, FO, and NF processes [9,10].

MD has extensively been explored at the laboratory scale with few applications in pilot scales for water desalination and wastewater treatment [11–13]. For this reason, further studies that include process efficiency, fouling mitigation, and cost analysis should be conducted to scale-up MD to an industrial level [14,15]. MD is currently affected by three factors: (i) wettability, (ii) fouling, and (iii) low water recovery rates [16,17]. These factors limit the choice of suitable polymers for MD applications. To mitigate the challenges associated with MD, extensive

* Corresponding author at: Department of Chemical, Metallurgical and Material Engineering, Tshwane University of Technology, Private Bag x680, Pretoria, 0001, South Africa.
E-mail address: nthunyalebea@gmail.com (L.N. Nthunya).

https://doi.org/10.1016/j.jece.2020.103654
Received 14 October 2019; Received in revised form 8 December 2019; Accepted 1 January 2020
Available online 07 January 2020
2213-3437/

research has been conducted on PVDF, which is characterized by low wetting propensities [18,19].

PVDF membranes used in MD are commonly designed as flat sheets, hollow fibers, and nanofibrous membranes. To further enhance their hydrophobicity for improved applications in MD, nanoparticles (e.g., SiO_2NPs) have been incorporated into PVDF membranes [20,21]. For example, Wang et al. synthetized amphiphilic membranes consisting of SiO_2NPs, chitosan hydrogel, and fluoro-polymer for the separation of oil from water [22]. These modified membranes exhibited better performances compared to commercial PVDF membranes. Other study included the use of alcohol as a non-solvent during phase inversion process leading to the formation of super-hydrophobic PVDF membrane [19].

In addition to wetting resistance, lotus effect (self-cleaning process) is yet another milestone to be achieved for the prevention of membrane fouling [23]. Through lotus effect, membranes achieve high contact angles close to 180° and low sliding angle (≤10°), providing an efficient foulant removal from the membrane surface [24,25]. Samaha et al. grafted SiO_2NPs on PVDF membranes to mimic this lotus effect [26]. The water-membrane contact angle (~160°) observed in this previous study was comparably similar to other studies reporting super-hydrophobic and low-fouling membranes [19,20,26–28]. Despite the extensive research and recent breakthroughs achieved in MD, fouling remains the critical challenge. Although fouling has been established in MD applications, further research studies focusing on innovative low-fouling superhydrophobic PVDF nanofibre membranes is imperative.

The fouling studies reported in MD are dominated by organic and inorganic fouling [29,30]. The hydrophobic nature of the membrane promotes chemical interactions with inorganic, colloids, organics macromolecules which inevitably accumulates on the surface or internal structures of the membrane [31]. Therefore, fouling promotes wetting, and consequently decreases the overall performance of the membrane [32,33]. In addition to colloidal, organic, and inorganic fouling, biofouling has been observed in MD. However, research on biofouling in MD is slowly growing [34], mainly influenced by the perception that the operating conditions, e.g., high operating temperatures (≥60°) and saline feed waters, do not allow the growth and accumulation of bacteria [34]. Nevertheless, some wastewaters discharged from thermophilic bioreactor systems find their way into natural aquifers [35–38]. A previous study by Frock et al. demostrated the existence of thermophilic bacteria in marine environments, hot springs, hydrothermal vents, and open surface waters; indicating their potential occurrence in MD processes [39]. Therefore, further studies on the mitigation of biofouling in MD while maintaining high wetting resistances and recovery rates is of paramount importance.

In this study, superhydrophobic SiO_2NPs-embedded PVDF nanofibre membranes were prepared. Their fouling resistances were tested in DCMD mode. These SiO_2NPs were further modified using three silane reagents: octadecyltrimethoxysilane (OTMS), N-octadecyltrichlorosilane (ODTS), and chlorodimethyl-octadecyl silane (Cl-DMOS). These silane reagents were characterized by long bulky chain and hydrophobic alkyl groups that form self-assembled layers on silicon dioxides [40–42]. These silane agents have not been explored in the preparation of SiO_2NPs-incorporated PVDF nanofibre membranes for MD processes [40–42]. Furthermore, the superhydrophobic SiO_2NPs-embedded PVDF nanofibre membranes were coated using a hydrophilic thin layer impregnated with carboxylated multiwalled carbon nanotubes (f-MWCNTs) and silver nanoparticles (AgNPs) to induce membrane fouling resistance towards thermophilic bacteria, colloidal, and organic fouling [43,44]. Certainly, the hydrophilic coating layer would provide a promising approach and research direction for organic, colloidal, and biofouling mitigation in DCMD processes.

2. Methods

2.1. Reagents

Polyvinylidene fluoride (PVDF) (MW = 534,000 g.mol^{-1}), tetraethyl orthosilicate (TEOS) (reagent grade, 98 %), *N,N*-dimetheylacetamide (DMAc) (Puriss p.a., 99.5 %), acetone (ACS reagent, 99.5 %), absolute ethanol (ACS reagent, 99.9 %), toluene (ACS reagent, 99.7 %), octadecyltrimethoxysilane (OTMS) (technical grade, 90 %), sodium alginate (medium viscosity), LUDOX® AS-40 colloidal silica (40 wt. % suspension in H_2O), and a 30 mL PP/PE eccentric syringe equipped with a blunt tip dispensing needle were purchased from Sigma Aldrich (Germany). N-octadecyltrichlorosilane (ODTS) (reagent grade, 95 %) and chlorodimethyl-octadecyl silane (Cl-DMOS) (reagent grade, 95 %) were purchased from Alpha Aesar (USA). Granny Smith apple extract were purchased from Makolobane Farmers Enterprises (South Africa). Deionized water (Direct-Q®, Merck Millipore) was used for solution preparation.

3. Experimental

3.1. Synthesis of SiO_2NPs

SiO_2NPs were prepared using a simplified green chemical reduction method that involved the use of apple extract as a reducing agent. Briefly, 0.05 M NaOH (50 µL), apple extract (10 mL) and ethanol (25 mL) were ultrasonicated in a flask for 2 h. Subsequently, TEOS (2 mL) was added to the flask and ultrasonication was continued for 5. The obtained SiO_2NPs were rinsed with ethanol and dried. The SiO_2NPs were modified using silane reagent (ODTS, OTMS, or Cl-DMOS) as reported in the literature [45].

Synthesis of PVDF nanofibre membranes

Nanofibre membranes were synthesized using an electrospinning technique adopting previously reported parameters / conditions [38,46,47]. Briefly, 15 % (w/v) PVDF was transferred to a 30 mL plastic syringe fitted with a 0.8 mm internal diameter needle. The syringe was placed on a single syringe pump. A high voltage generator was used to induce an electric field between the collecting plate and the tip of the needle. The positive terminal of the DC generator was connected to the tip of the syringe needle and the negative terminal was connected to the aluminium foil (rotating collecting plate). The nanofibres were synthesized under the following optimized electrospinning conditions: syringe injection flow rate of 1.0 mL/h, distance of 14 cm between the aluminium foil and the tip of the needle, and a voltage of 23 kV at room temperature. The electrospun PVDF nanofibres were dried in an oven at 40 °C for 24 h to remove moisture. Also, PVDF nanofibre membranes were embedded with 1.0 % (w/v) organically-modified SiO_2NPs (i.e., ODTS-modified, OTMS-modified, or Cl-DMOS-modified SiO_2NPs) to enhance their super-hydrophobicity by blending the PVDF solution with 1.0 % (w/v) SiO_2NPs and electrospun in situ. The superhydrophobic PVDF nanofibre membranes were coated using 2 % AgNPs and 1 % f-MWCNTs to produce an antibacterial and hydrophilic thin layer. The modification procedure was reported elsewhere [48]. The uncoated membranes: (M1) pristine PVDF, (M2) SiO_2NPs-modified PVDF, (M3) ODTS-functionalised SiO_2NPs-modified PVDF; (M4) OTMS-functionalised SiO_2NPs-modified PVDF, (M5) Cl-DMOS-functionalised SiO_2NPs-modified PVDF and coated membranes: (M6) coated pristine, (7) coated SiO_2NPs-modified PVDF, (M8) coated ODTS-functionalised SiO_2NPs-modified, and (M9) coated OTMS-functionalised SiO_2NPs-modified PVDF, (M10) coated Cl-DMOS-functionalised SiO_2NPs-modified PVDF nanofibre membranes were dried in an oven for 24 h before experiments. OTMS-functionalised SiO_2 improved the contact angles of the PVDF nanofibres membranes and they are therefore referred as the f-SiO_2NPs throughout the entire manuscript. The nomenclature of the synthesised membranes was summarised in Table 1.

Table 1
Nomenclature and composition of the pristine and modified PVDF membranes used in the current study. The concentration of the additives was reported relative to the amount of PVDF.

Membranes	Polymer	SiO_2NPs	ODTS-SiO_2NPs	OTMS- SiO_2NPs	Cl-DMOS-SiO_2NPs	Coating layer containing both f-MWCNTs and AgNPs	
						f-MWCNTs	AgNPs
M1	PVDF	–	–	–	–	–	–
M2	PVDF	1 %	–	–	–	–	–
M3	PVDF	–	1 %	–	–	–	–
M4	PVDF	–	–	1 %	–	–	–
M5	PVDF	–	–	–	1 %	–	–
M6	PVDF	–	–	–	–	1 %	2 %
M7	PVDF	1 %	–	–	–	1 %	2 %
M8	PVDF	–	1 %	–	–	1 %	2 %
M9	PVDF	–	–	1 %	–	1 %	2 %
M10	PVDF	–	–	–	1 %	1 %	2 %

3.2. Characterization of virgin and fouled nanofibre membranes

The morphology of virgin and fouled PVDF nanofibre membranes was investigated using Scanning Electron Microscope (SEM, JOEL STM – IT300). The samples were fixed on a conductive carbon tape and carbon-coated. Energy-dispersive X-ray Spectroscopy (EDS) was used to investigate the elemental composition of the membranes. In addition, the surface roughness of the membranes was studied using atomic force microscopy (AFM, Witec Alpha 300 A, TS-150). The membranes were scanned in an area of 10.0 μm × 10.0 μm. The membranes fouled with biofilms were prepared for confocal microscopy using an in-house protocol. Live/dead cells were visualized using a Nikon A1R laser scanning microscope. The samples were placed in a sterile petri dishes immediately after removal from the operating MD module and stained with the Live/Dead Bac Light Bacterial Viability and the results were reported elsewhere [48]. The water contact angle (CA) of the PVDF membranes was measured using a DSA3OE Kruss drop shape analyser (GmbH) on virgin and fouled membranes by the sessile drop method. 5 μL of probe liquids was used in all experiments. To determine the surface energy (surface tension) component of the membranes, the contact angles were determined with three well-characterized probe liquids (de-ionized water, glycerol and diiodomethane). Diiodomethane was used as the dispersive (non-polar) liquid while de-ionized water and glycerol were used as polar liquids. The interfacial free energy for interaction between the membrane (m) and the solute or foulant (s) in water (w) was estimated adopting the previously reported equations [9,49,50]. (See the SI for further descriptions)

$$\Delta G^{D}_{swm} = 2(\sqrt{\sigma^{D}_{w}} - \sqrt{\sigma^{D}_{s}})(\sqrt{\sigma^{D}_{m}} - \sqrt{\sigma^{D}_{w}}) \quad (1)$$

$$\Delta G^{P}_{swm} = 2\sqrt{\sigma^{+}_{w}}(\sqrt{\sigma^{-}_{s}} + \sqrt{\sigma^{-}_{m}} - \sqrt{\sigma^{-}_{w}}) + 2\sqrt{\sigma^{-}_{w}}(\sqrt{\sigma^{+}_{s}} + \sqrt{\sigma^{+}_{m}} - \sqrt{\sigma^{+}_{w}}) - 2\sqrt{\sigma^{+}_{s}\sigma^{-}_{m}} - 2\sqrt{\sigma^{-}_{s}\sigma^{+}_{m}} \quad (2)$$

$$\Delta G^{TOT}_{swm} = \Delta G^{D}_{swm} + \Delta G^{P}_{swm} \quad (3)$$

Where ΔG^{TOT}_{swm} is the total free energy of cohesion.

3.3. Preparation of the feed solutions

3.3.1. Sodium alginate and colloidal silica as model organic and colloidal foulants

The test solution was composed of 5.0 mg/L $CaCl_2$ and 20 mg/L sodium alginate. NaCl was added to the feed solution until a 47 mS/cm conductivity was attained. The feed solution containing colloidal silica was prepared as follows. $CaCl_2$ and colloidal silica were added to de-ionized water at 5.0 mg/L and 40 wt%, respectively. NaCl was further added to this feed solution to attain a total ionic conductivity of 47 mS/cm. The feed solutions were sonicated prior to use.

3.3.2. Model bio-foulants

Feed solutions used for biofouling tests were collected from the thermophilic bacteria effluent at Innolab Company (Ghent, Belgium). The plastic containers used to collect the water samples were rinsed three times with the water from the effluent prior to collection. The samples were pretreated by a 10 μm filter (Millipore Isopore, TCTP). The filters were continuously replaced to mitigate any cake formation. Calcium chloride ($CaCl_2$) was added to the pretreated solution to reach a final concentration of 5.0 mg/L. Furthermore, sodium chloride was added to the pretreated solution until a 47 mS/cm total ionic conductivity of the feed solution was achieved.

3.4. Performance of the PVDF nanofibre membranes

The performance of the PVDF nanofibre membranes embedded with organically-modified SiO_2NPs was tested on a DCMD lab-scale set-up using a solution characterized by the model foulants presented earlier. The total ionic conductivity of each solution was adjusted to 47 mS/cm using NaCl (i.e., slightly below the concentration of dissolved salts in seawater). The temperature of the feed was 60 °C while the permeate temperature was kept constant at 20 °C in counter mode. A flow rate of 0.75 L/min was set for feed solution and the coolant water (conductivity ≤ 0.10 μS/cm). The conductivity of the water was measured using a Shimadzu conductivity meter to determine the salt rejection efficiencies. The water flux was calculated based on the mass of water transported from the feed (i.e., modified PVDF membrane; surface area: 1.25×10^{-2} m^2) to the permeate. The amount of water transported through the membrane in the state of vapour was determined by measuring the weight increment of the coolant water using a Kern & Sohn GmbH, EMB 3000_1 weighing balance. The following Eq. (1) was used to calculate the water flux (J_{water}):

$$\text{Jwater} = \frac{\Delta V}{\Delta t.\ A} \quad (1)$$

where ΔV was the volume of the permeate collected at a time interval Δt, and Am was the membrane surface area. The difference in volume (ΔV) of the water collected was calculated from the change in mass (Δm) of the water collected (Eq. 2), where 0.997 kg/L was used as the density (ρ) of water at room temperature.

$$\Delta\ \text{V} = \frac{\Delta m}{\rho} \quad (2)$$

A new nomenclature of fouled nanofibre membranes was developed as follows: colloidal fouling on (M1) pristine PVDF, (M2) f-SiO_2NPs-modified PVDF and (M3) coated f-SiO_2NPs-modified PVDF; biofouling on (M4) pristine PVDF, (M5) f-SiO_2NPs-modified PVDF and (M6) coated f-SiO_2NPs-modified PVDF; alginate fouling on (M7) pristine PVDF, (M8) f-SiO_2NPs-modified PVDF and (M9) coated f-SiO_2NPs-modified PVDF. A summary of the new nomenclature and composition of the fouled membrane is provided in Table 2.

Table 2
Nomenclature and composition of fouled membranes.

Fouling type	Membrane	Polymer	Hydrophobic additives	Coating layer Hydrophilic/ antimicrobial additives	
			f-SiO_2NPs	f-MWCNTs	AgNPs
Colloidal-fouled	M1	PVDF	–	–	–
	M2	PVDF	1 %	–	–
	M3	PVDF	1 %	1 %	2 %
Bio-fouled	M4	PVDF	–	–	–
	M5	PVDF	1 %	–	–
	M6	PVDF	1 %	1 %	2 %
Alginate-fouled	M7	PVDF	–	–	–
	M8	PVDF	1 %	–	–
	M9	PVDF	1 %	1 %	2 %

4. Results and discussion

4.1. SEM-EDS analysis of the fouled membranes

The cake formation leading to membrane fouling was investigated using SEM analysis. Colloidal silica, sodium alginate, and the effluent from the thermophilic bacteria bioreactor were used as model inorganic, organic, and bacterial fouling. Ca^{2+} ions were added to feed solutions containing the model foulants owing to their cation bridging formation potential (i.e., inner-sphere complexation) between ionized functional groups on foulants and membranes; thus, leading to high fouling propensities as previously reported [51–53]. After 50 h of operation, the membranes were characterized by layer formation and deposition of the particulate matter. The colloidal silica particles were deposited in the internal microstructures of PVDF nanofibres membranes; while their deposition was lower on its hydrophilic thin layer-coated counterpart (Fig. 1, M1 and M2). The SEM micrographs revealed a severe cake formation on both alginate and bio-fouled pristine PVDF and f-SiO_2NPs-modified PVDF nanofibre membranes (Fig. 1, M4, M5, M7 and M8). A similar observation was also reported by Zarebska and co-workers [54]. The cake formation was significantly lower in all hydrophilic thin layer-coated membranes, suggesting minimal fouling occurring on the surface of the membrane (Fig.1, M3, M6 and M9). The investigated bio-fouled membranes were characterized by rod-like structures, which indicate the presence of bacteria on the surface of the membranes.

Remarkably, the surface of pristine PVDF and f-SiO_2NPs-modified PVDF nanofibre membranes were fully covered by a cake layer of alginate and biofilms. However, the f-MWCNTs/AgNPs coating significantly reduced the deposition and cake formation on the surface of the membrane. The cross-section of membranes was recorded to elucidate the degree of cake formation on the fouled membranes. The rejection studies on section 3.6 showed the highest flux decline on membranes subjected to alginate fouling. The cross-section of membrane samples highly impacted by fouling (Fig. 2) showed a 53 nm thickness layer on the membrane surface. The thickness of the cake layer is rarely reported on literature in MD. However, fouling experiments conducted on humic acid in electro-coagulation/oxidation membrane reported the formation of cake layer with thickness ≈ 30 nm [55]. In this study, the cake formation resulted in a 90 % flux decay on f-SiO_2NPs-modified PVDF nanofibre membrane (section 3.6). Fig. 2 (M2) shows the cross-section of coated f-SiO_2NPs subjected to alginate solution in DCMD. Clearly, membrane coating significantly reduced cake formation due to lower membrane surface roughness and hydrophobicity. Furthermore, alginate was unable to interact with silanol groups and causing cake formation [51].

4.2. EDS analysis of fouled membranes

The EDX spectra (i.e., elemental components) on fouled membranes were presented on Fig. 3. The following elements were identified in colloidal silica-fouled pristine PVDF nanofibre membrane: C, O, F, Na, Si, Cl, and Ca, which are the elemental components of pristine PVDF nanofibre membranes and feed solution (Fig. 3, M1). Similarly, these elements were observed on biofouled f-SiO_2NPs-modified PVDF nanofibre membranes (Fig. 3, M8). Additionally, elemental Ag was observed on the hydrophilic thin layer-coated membranes, which plays a key anti-bacterial fouling role (Fig. 3, M6).

4.3. AFM analysis of fouled membranes

The surface morphology of fouled membranes was studied using AFM. The arithmetic mean height (SA) and the root mean square height (SQ) of the voids on the surface of each membrane were used to estimate the effect of fouling towards membrane surface roughness. The SA values of M1, M2, M3, M4, M5, M6, M7, M8, M9 were 154 nm, 238 nm, 47 nm, 81 nm, 79 nm, 34 nm, 73 nm, 96 nm, and 41 nm, respectively (Fig. 4). The SA and SQ values of colloidal silica-fouled membranes were slightly higher than those of virgin membranes reported elsewhere [45]. This observation was supported by the deposition of colloidal particles presented on SEM micrographs. However, the SA and SQ values of alginate-fouled and bio-fouled membranes were lower than those of their previously reported virgin membranes counterpart [45], indicating that alginate and bio-foulants formed a smooth layer at the surface of the membranes. During membrane drying, cracks were recorded on fouled membranes by AFM images (typically in M4, M5, M7, and M8). Furthermore, the nanofibre membrane coating using a solution containing f-MWCNTs and AgNPs decreased the surface roughness of the fouled membranes. These observations are in good agreement with previously reported studies [19,56–58].

4.4. Contact angles of fouled membranes

The impact of fouling on membrane hydrophobicity was investigated using contact angles of virgin and fouled membranes. The results are presented in Table 3. The foulants (i.e. colloidal silica, alginate, and biological communities) showed different impacts towards membrane hydrophobicity. The contact angles of the virgin membranes (membranes before MD experiments) on M1, M2, and M3 were presented in the supplementary information (SI). There was no significant difference between the contact angles of the membranes fouled by colloidal silica and the virgin membranes. However, the membranes fouled by alginate showed a decrease in hydrophobicity. The contact angles were measured as 84 ± 6°, 147 ± 7°, and 63 ± 4° on M7, M8, and M9 respectively. Likewise, the contact angles of membranes fouled by biological communities changed to 96 ± 3°, 164 ± 8°, and 67 ± 3° on M4, M5, and M6 respectively. A decrease in membrane contact angles induced by the accumulation of alginate would be ascribed to the hydrophilic moieties (COO^- and $-OH$) present in alginate [59,60]. However, the contact angles of membranes fouled by biological communities were either slightly lower on coated f-SiO_2-modified PVDF nanofibre membranes or also higher on f-SiO_2-modified PVDF nanofibre membranes. The cell membranes of most bacteria are characterized by amphipathic phospholipids containing a hydrophobic tail and a hydrophilic head [61]. Furthermore, bacteria properties range from hydrophilicity to hydrophobicity, which inevitably influences the hydrophobic nature of the membrane by either lowering or increasing the membrane contact angles [62,63]. The impact of fouling on membrane hydrophobicity has been widely reported in previous studies and is consistent with the findings of this current research [30,55,64,65].

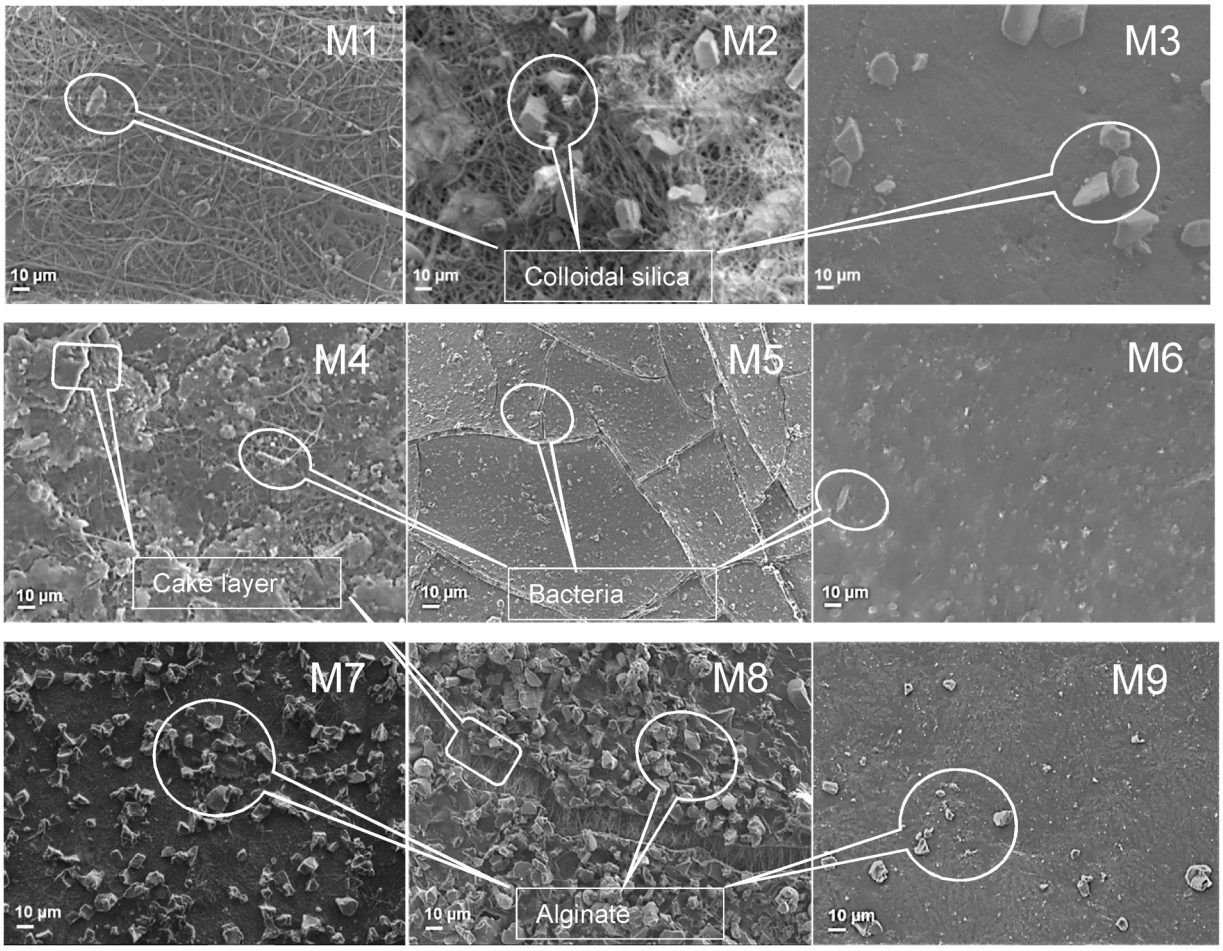

Fig. 1. SEM images of: colloidal silica fouling on (M1) pristine PVDF nanofibre, (M2) f-SiO_2NPs-modified PVDF nanofibre, and (M3) thin hydrophilic layer-coated PVDF nanofibre membrane; biofouling on (M4) pristine PVDF nanofibre, (M5) f-SiO_2NPs-modified PVDF nanofibre, and (M6) thin hydrophilic layer-coated PVDF nanofibre membrane; and alginate fouling on (M7) pristine PVDF nanofibre, (M8) f-SiO_2NPs-modified PVDF nanofibre, and (M9) thin hydrophilic layer-coated PVDF nanofibre membrane.

4.5. Determination of membrane-foulant interfacial free energy

The contact angles of fouled membranes were measured using three probe liquids to calculate the interfacial free energy between membranes and solutes (foulants) and the results are presented in Table 4. The fouling on the membrane lowered the surface free energy of the dispersive components below that of the polar components, suggesting a clear modification of the membrane [66]. Furthermore, the interfacial free energies (ΔG) between the membrane and foulants were calculated and tabulated in Table 4. The negative values of ΔG indicated that the attractive interaction between membranes and foulants was favourable [51]. These membranes-foulants attractive interactions led to a decline in water flux, suggesting that long-term operations would not be ideal due to a decrease in water permeability.

4.6. Effect of membrane fouling on water flux and salt rejection

Fouling is a major problem that affects all membrane-based processes. It is defined as the accumulation of the solutes on the surface of the membrane during separation [30]. The model foulants studied were colloidal silica and alginic salt of sodium. The effect of biofouling on MD was reported elsewhere [48]. Generally, all model foulants induced

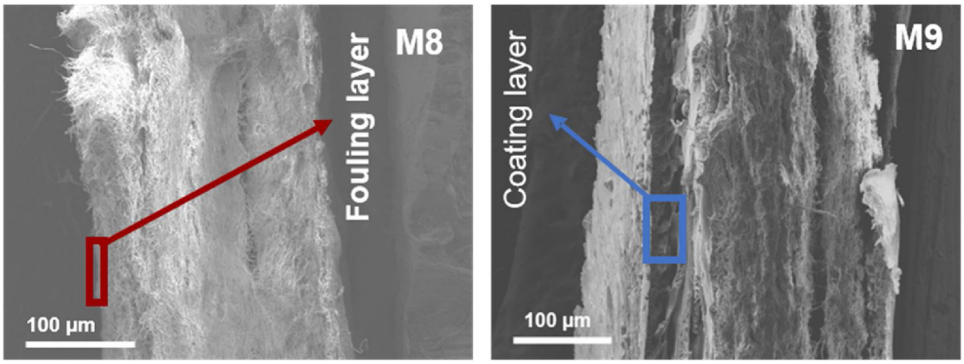

Fig. 2. Cross-sectional view of alginate-fouled membranes: (M8) f-SiO_2NPs-modified PVDF and (M9) coated f-SiO_2NPs-modified PVDF nanofibre membranes.

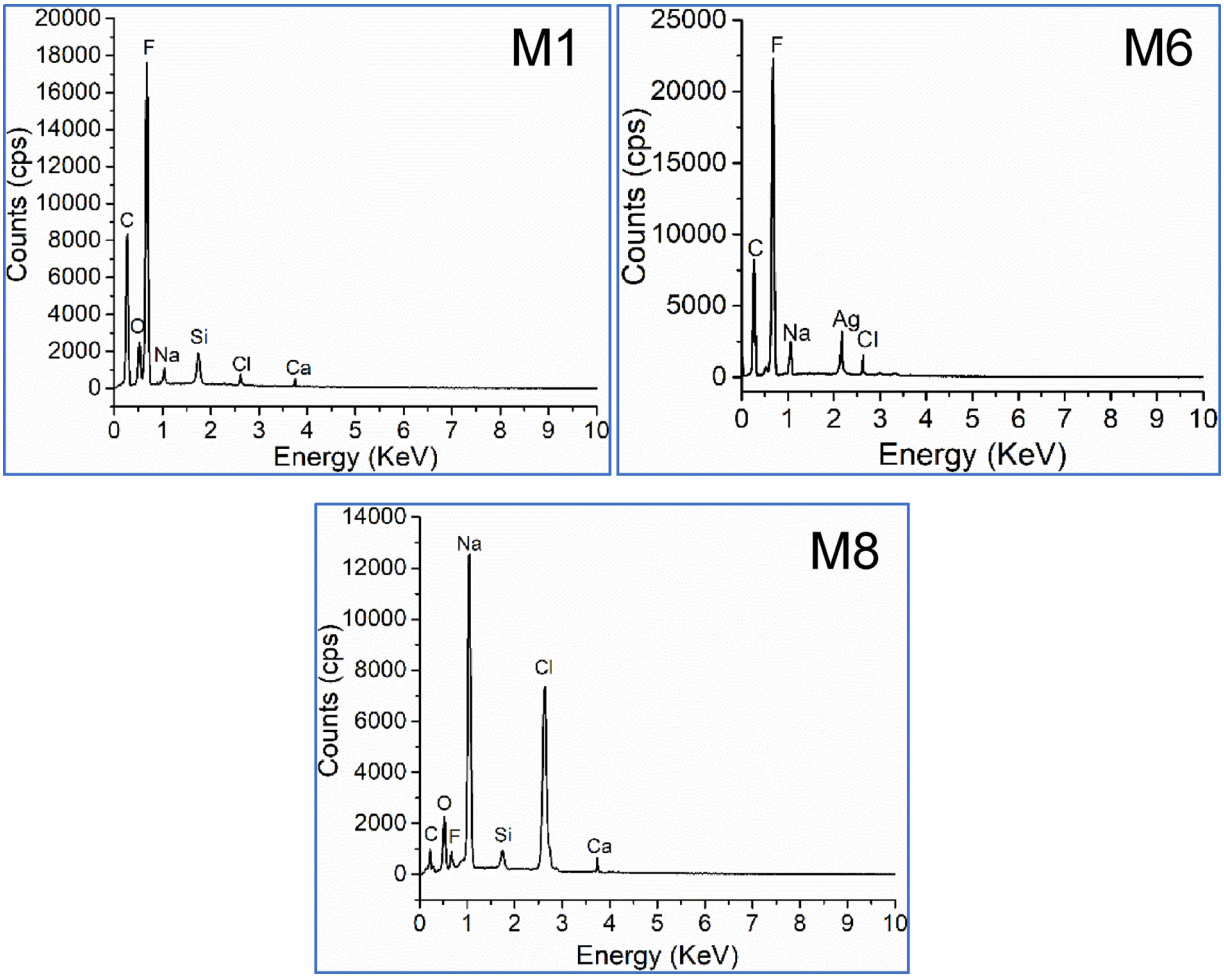

Fig. 3. EDX spectra of: (M1) colloidal silica-fouled pristine PVDF nanofibre membrane, (M6) biofouling on coated PVDF nanofibre membrane, and (M8) alginate-fouled f-SiO_2NPs-modified PVDF nanofibre membrane.

a decline in water flux as well as a decay in salt rejection (Fig. 5). The fouling profile demonstrated that alginate-fouling resulted in a drastic water flux decay (64.93–90.37 %) compared to a moderate decay caused by colloidal fouling (30.34–44.42 %) (Fig.5, M1–5). Fouling intensification on SiO_2NPs-modified PVDFs nanofibre was induced by silanol-alginate interactions where bridge formation between the membrane and the alginate was induced by the presence of Ca^{2+} ions [51]. The SEM results showed a cake formation of alginate and growth of biofilms on the membrane surface, which are the key explanations for the deterioration of the water flux within the first 50 h of operation. These observations were also reported by Zarebska and co-workers [54]. Furthermore, colloidal silica particles penetrate into the membrane pores, causing a severe pore blockage in flat sheet membranes [67]. However, due to the bigger pore sizes (1–2.5 μm) in nanofibre membrane, the colloidal silica particles have little effect on the decrease of water flux. The decay in salt rejection efficiency is an evidence of membrane wetting which subsequently decreases the quality of the permeate. The effect of the foulants towards the rejection decays followed the order of: alginate (6.13–6.87 %) > colloidal silica (1.42–2.48 %) (Fig. 5, M1–5). These observations were consistent to previously reported studies [30,33,54,64,68]. A sustainable MD performance was observed during the use of coated membrane where both flux and salt rejection efficiencies remained almost stable in the first 50 h of operation. Remarkably, a rejection efficiency below 99 % in MD is an indication of an inefficient process. In this case, the flux decay induced by alginate and colloidal silica were 24.22–36.87 % and 10.39–15.60 % respectively (Fig. 5, M6–10). On the other hand, the rejection decays were 0.75–1.04 % and 0.07-0.16 % due to alginate and colloidal fouling, respectively. The oxidized MWCNTs and AgNPs coating of the surface rendered the superhydrophobic PVDF membranes resistant to adhesion of microbiological communities [48] while preventing silanol-alginate interactions. These findings were also evidenced by previously reported literature, where membrane fouling caused decays in water flux and rejection efficiencies during the oil-water separation and water desalination [69,70].

5. Conclusion

In our previous study, it was demonstrated that incorporation of the f-SiO_2NPs successfully improved the hydrophobicity of PVDF nanofibre membranes. SiO_2NPs were modified using three silane reagents, namely; ODTS, OTMS, and Cl-DMOS. The contact angles reported increased from 94° to 156-162°. To mitigate fouling propensities of the membrane while maintaining membrane resistance to wetting, the superhydrophobic membranes were coated with a thin layer layer containing f-MWCNTs and AgNPs. The hydrophobic membranes were characterized by formation of a cake layer induced by the alginate and biofoulings. Furthermore, particulate colloids were deposited on the surface of the uncoated membranes. Remarkably, cake formation formed a smooth topology on the surface of the membrane while colloidal silica increased membrane surface roughness above the surface roughness of their counter-part virgin membranes. It was observed that, membrane coating reduced the cake formation. Furthermore, the presence of the AgNPs on the coating layer inhibited the growth of micro-

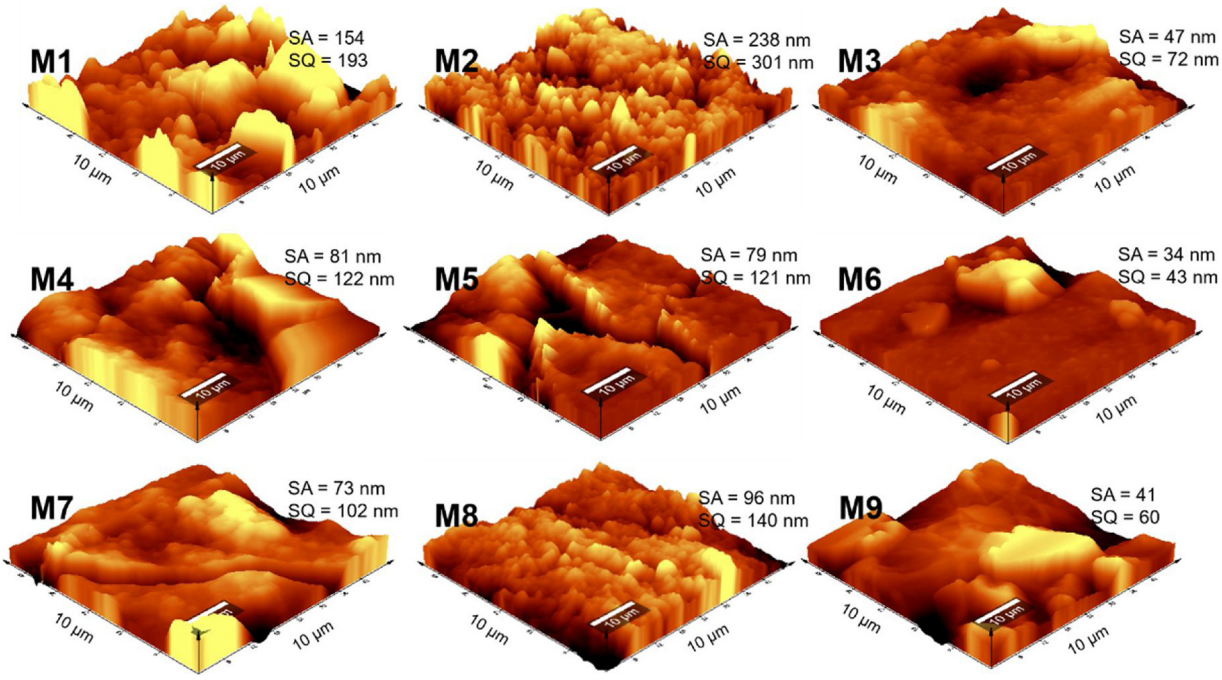

Fig. 4. AFM images of fouled membranes: colloidal silica fouling on (M1) pristine PVDF nanofibre, (M2) f-SiO_2NPs-modified PVDF nanofibre, and (M3) thin hydrophilic layer-coated PVDF nanofibre membranes; biofouling on (M4) pristine PVDF nanofibre, (M5) f-SiO_2NPs-modified PVDF nanofibre, and (M6) thin hydrophilic layer-coated PVDF nanofibre membrane; and alginate fouling on (M7) pristine PVDF nanofibre, (M8) f-SiO_2NPs-modified PVDF nanofibre, and (M9) thin hydrophilic layer-coated PVDF nanofibre membrane.

Table 3
Contact angles of fouled membranes.

Type of fouling	Membrane	Contact angle (°)
Colloidal-fouled	M1	94 ± 6
	M2	155 ± 11
	M3	69 ± 5
Bio-fouled	M4	96 ± 4
	M5	164 ± 8
	M6	67 ± 3
Alginate-fouled	M7	84 ± 3
	M8	147 ± 7
	M9	63 ± 4

Colloidal fouling on (M1) pristine PVDF nanofibre, (M2) f-SiO_2NPs-modified PVDF nanofibre, and (M3) thin hydrophilic layer-coated PVDF nanofibre membranes; biofouling on (M4) pristine PVDF nanofibre, (M5) f-SiO_2NPs-modified PVDF nanofibre, and (M6) thin hydrophilic layer-coated PVDF nanofibre membrane; and alginate fouling on (M7) pristine PVDF nanofibre, (M8) f-SiO_2NPs-modified PVDF nanofibre, and (M9) thin hydrophilic layer-coated PVDF nanofibre membrane.

organisms, hence improved membrane resistance towards bio-fouling. The contact angles of the fouled membranes were used to estimate the type of interactions between the membranes and the foulants. It was observed that, alginate slightly decreased the membrane contact angles while biofoulings and colloidal silica slightly increased the water-membrane contact angles. The interfacial free energies values were all negative, indicating that the membranes-foulants interactions were attractive. This phenomeno agreed with SEM micrographs, which demonstrated the formation of a cake layer on the surface of the membranes. Consequently, the 30–90 flux decays were recorded within 50 h of operation. Furthermore, salt rejections were reduced by 1.4–6.1 %. Although, membrane coating decreased the initial water flux from 43 to 45 LMH to 16-17LMH, stable water fluxes were observed within 50 h of operation where the decays of 19–31 % flux decays were recorded.

Table 4
Membranes-foulants interfacial free energy determining the initial membrane fouling.

Interactive type		Surface free energy components			ΔG (mJ/m^2)
		σ_s^- (mJ/m^2)	σ_s^+ (mJ/m^2)	σ_s^D (mJ/m^2)	
Colloidal					
	M1	12.1	1.62	0.0004	−9.9
	M2	15.2	0.38	0.044	−7.3
	M3	10.9	1.62	0.028	−67.0
Biological					
	M4	9.54	2.24	1.04	−19.6
	M5	5.69	7.40	1.04	−44.3
	M6	9.87	1.08	0.004	−83.6
	M7	14.9	0.25	0.01	−36.4
	M8	16.0	0.11	0.06	−3.9
	M9	8.61	0.97	0.66	−56.1

σ_s^- = base component of the surface energy of the solid, σ_s^+ = acid component of the surface energy of the solid, σ_s^D = dispersive component of the surface energy of the solid, ΔG = Interfacial free energy; colloidal fouling on (M1) pristine PVDF nanofibre, (M2) f-SiO_2NPs-modified PVDF nanofibre, and (M3) thin hydrophilic layer-coated PVDF nanofibre membranes; biofouling on (M4) pristine PVDF nanofibre, (M5) f-SiO_2NPs-modified PVDF nanofibre, and (M6) thin hydrophilic layer-coated PVDF nanofibre membrane; and alginate fouling on (M7) pristine PVDF nanofibre, (M8) f-SiO_2NPs-modified PVDF nanofibre, and (M9) thin hydrophilic layer-coated PVDF nanofibre membrane.

Auspiciously, the stable salt rejections were observed with 0.1–1.0 % rejection decays recorded. Although, these results are an indication of a promising fouling and wetting mitigations in MD, further research is required to ensure non-occurrence of membrane wetting within the membrane pores. Additionally, long term operation conditions (a minimum of 600 h) are required to determine their effect towards membrane wetting. Nonetheless, this membrane modification showed possible development of fouling-resistant membrane to mitigate challenges associated with MD processes.

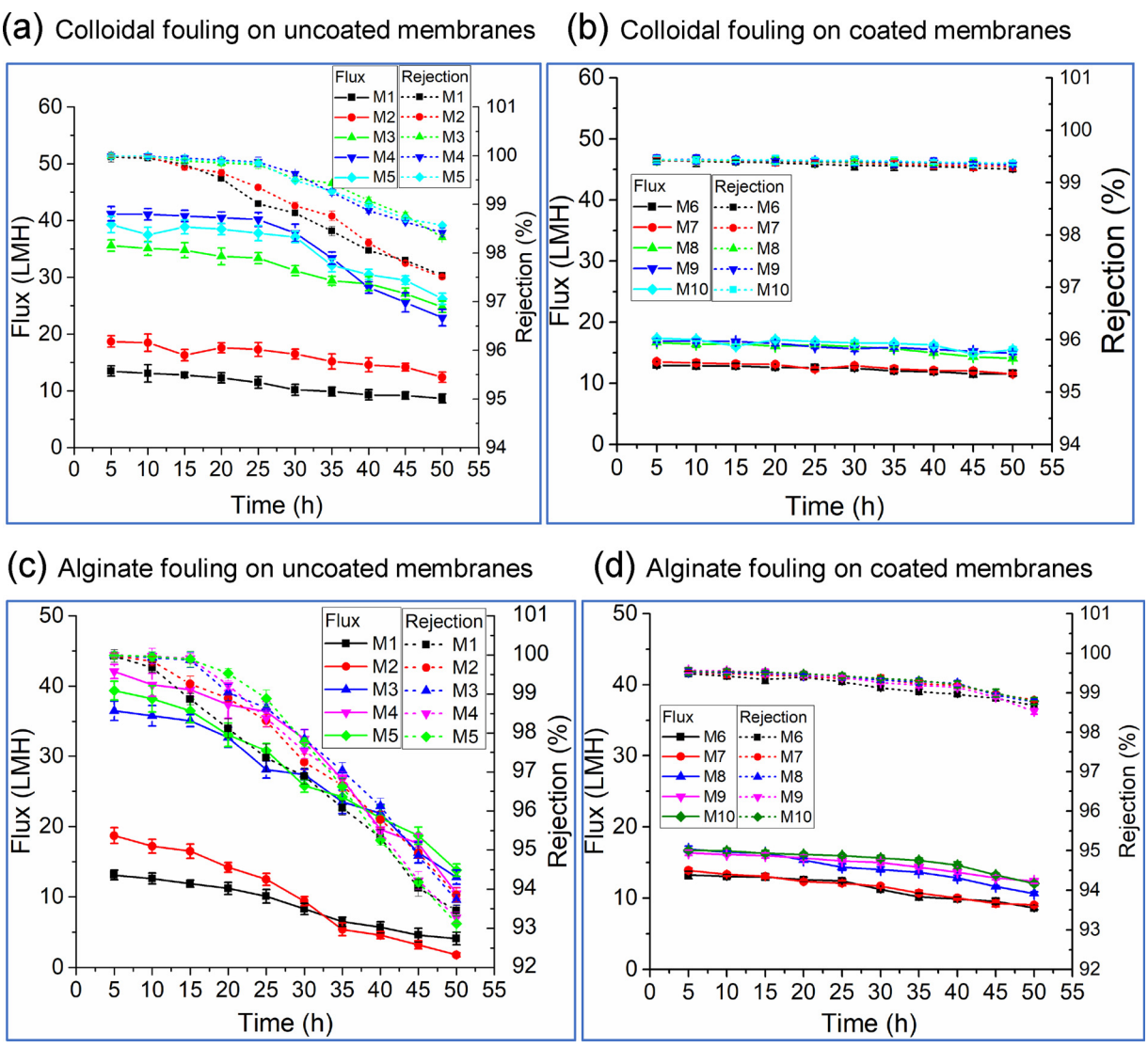

Fig. 5. Effect of colloidal and organic on MD permeate flux and salt rejection efficiency. Uncoated membranes: (M1) Pristine membrane, membrane modified with (M2) pristine SiO_2NPs, (M3) ODTS-functionalized SiO_2 NPs, (M4) OTMS-functionalized SiO_2NPs, and (M5) Cl-DMOS-functionalized SiO_2NPs; coated membranes: (M6) Pristine membrane, membrane modified with (M7) pristine SiO_2NPs, (M8) ODTS-functionalized SiO_2 NPs, (M9) OTMS-functionalized SiO_2NPs, and (M10) Cl-DMOS-functionalized SiO_2NPs.

CRediT authorship contribution statement

Lebea N. Nthunya: Data curation, Formal analysis, Investigation, Visualization, Writing - original draft. **Leonardo Gutierrez:** . **Edward N. Nxumalo:** Project administration, Resources, Software, Validation, Writing - review & editing. **Arne R. Verliefde:** Conceptualization, Funding acquisition, Project administration, Resources, Supervision, Writing - review & editing. **Sabelo D. Mhlanga:** Conceptualization, Funding acquisition, Project administration, Resources, Supervision, Writing - review & editing. **Maurice S. Onyango:** Funding acquisition, Project administration, Resources, Validation, Writing - review & editing.

Declaration of Competing Interest

All authors have read the revised manuscript and have approved to resubmit it. In addition, all the authors confirm that: “the manuscript, or its contents in some other form, has not been published previously by any of the authors and/or is not under consideration for publication in another journal at the time of submission”. Finally, the authors declare no conflict of interest.

Acknowledgements

The authors would like to thank the National Research Foundation, Tshwane University of Technology, University of South Africa and Ghent University for funding this work.

Appendix A. Supplementary data

Supplementary material related to this article can be found, in the online version, at doi:https://doi.org/10.1016/j.jece.2020.103654.

References

[1] R.K. Mishra, S.C. Dubey, Fresh water availability and it’s global challenge, Int. J. Eng. Sci. Invent. Res. Dev. 2 (2015) 351–407.
[2] A.Y. Hoekstra, M.M. Mekonnen, A.K. Chapagain, R.E. Mathews, B.D. Richter, Global monthly water scarcity: Blue water footprints versus blue water availability, PLoS One 7 (2012) 1–9, https://doi.org/10.1371/journal.pone.0032688.
[3] L.N. Nthunya, N.P. Khumalo, A.R. Verliefde, B.B. Mamba, S.D. Mhlanga, Quantitative analysis of phenols and PAHs in the Nandoni Dam in Limpopo Province, South Africa: A preliminary study for Dam water quality management, Phys. Chem. Earth, Parts A/B/C. (2019) 1–9, https://doi.org/10.1016/j.pce.2019.02.003.

[4] L.N. Nthunya, S. Maifadi, B. Mamba, A.R.Verliefde Bhekie, S.D. Mhlanga, Spectroscopic determination of water salinity in brackish surface water in Nandoni Dam, at Vhembe District, Limpopo Province, South Africa, Water. 10 (2018) 1–13, https://doi.org/10.3390/w10080990.

[5] C. Aydiner, D.Y.K. Imer, S. Oncel, E.C. Dogan, A.O. Narci, S. Cakmak, T.N. Yilmaz, E.E. Celebi, Y.M. Tilki, Marmara seawater desalination by membrane distillation: direct consumption assessment of produced drinking water, Desalination, INTECH, London, 2017, pp. 2–29, https://doi.org/10.5772/intechopen.68653.

[6] M.A. Salehi, R. Rostamani, Review of membrane distillation for the production of fresh water from saline water, J. Nov. Appl. Sci. 2 (2013) 1072–1075.

[7] G.M. Geise, H.S. Lee, D.J. Miller, B.D. Freeman, J.E. Mcgrath, D.R. Paul, Water purification by membranes: the role of polymer science, J. Polym. Sci. Part B Polym. Phys. 45 (2007) 1390–1398, https://doi.org/10.1002/polb.

[8] B. Singh, V. Kochkodan, R. Hashaikeh, N. Hilal, A review on membrane fabrication: structure, properties and performance relationship, Desalination 326 (2013) 77–95, https://doi.org/10.1016/j.desal.2013.06.016.

[9] L.N. Nthunya, L. Gutierrez, S. Derese, N. Edward, A.R. Verliefde, B. Mamba, S.D. Mhlanga, A review of nanoparticle-enhanced membrane distillation membranes : membrane synthesis and applications in water treatment, Chem. Technol. Biotechnol 94 (2019) 2757–2771, https://doi.org/10.1002/jctb.5977.

[10] K. He, H.J. Hwang, M.W. Woo, I.S. Moon, Production of drinking water from saline water by direct contact membrane distillation (DCMD), J. Ind. Eng. Chem. 17 (2011) 41–48, https://doi.org/10.1016/j.jiec.2010.10.007.

[11] L. Eykens, K. De Sitter, C. Dotremont, L. Pinoy, B. Van der Bruggen, Membrane synthesis for membrane distillation: a review, Sep. Purif. Technol. 182 (2017) 36–51, https://doi.org/10.1016/j.seppur.2017.03.035.

[12] B.L. Pangarkar, S.K. Deshmukh, M.V. Guddad, Economic assessment of multi-effect membrane distillation (MEMD) for water treatment, Int. J. Eng. Res. Technol. 10 (2017) 253–257.

[13] L. Song, Z. Ma, X. Liao, P.B. Kosaraju, J.R. Irish, K.K. Sirkar, Pilot plant studies of novel membranes and devices for direct contact membrane distillation-based desalination, J. Memb. Sci. 323 (2008) 257–270, https://doi.org/10.1016/j.memsci.2008.05.079.

[14] S. Al-obaidani, E. Curcio, F. Macedonio, G. Di, H. Al-hinai, E. Drioli, Potential of membrane distillation in seawater desalination: thermal efficiency, sensitivity study and cost estimation, J. Memb. Sci. 323 (2008) 85–98, https://doi.org/10.1016/j.memsci.2008.06.006.

[15] M. Khayet, Solar desalination by membrane distillation: dispersion in energy consumption analysis and water production costs (a review), Desalination 308 (2013) 89–101, https://doi.org/10.1016/j.desal.2012.07.010.

[16] F. Ardeshiri, A. Akbari, M. Peyravi, M. Jahanshahi, PDADMAC/PAA semi-IPN hydrogel-coated PVDF membrane for robust anti-wetting in membrane distillation, J. Ind. Eng. Chem. 74 (2019) 14–25, https://doi.org/10.1016/j.jiec.2019.01.035.

[17] Y. Shin, J. Sohn, Mechanisms for scale formation in simultaneous membrane distillation crystallization: effect of flow rate, J. Ind. Eng. Chem. 35 (2016) 318–324, https://doi.org/10.1016/j.jiec.2016.01.009.

[18] Y. Liao, R. Wang, M. Tian, C. Qiu, A.G. Fane, Fabrication of polyvinylidene fluoride (PVDF) nanofiber membranes by electro-spinning for direct contact membrane distillation, J. Memb. Sci. 425–426 (2013) 30–39, https://doi.org/10.1016/j.memsci.2012.09.023.

[19] S. Munirasu, F. Banat, A. Ahmed, M. Abu, Intrinsically superhydrophobic PVDF membrane by phase inversion for membrane distillation, Desalination 417 (2017) 77–86, https://doi.org/10.1016/j.desal.2017.05.019.

[20] Z.-Q. Dong, X.-H. Ma, Z.-L. Xu, Z.-Y. Gu, Superhydrophobic modification of PVDF–SiO2 electrospun nanofiber membranes for vacuum membrane distillation, RSC Adv. 5 (2015) 67962–67970, https://doi.org/10.1039/C5RA10575G.

[21] M. Sethupathy, V. Sethuraman, P. Manisankar, Preparation of PVDF/SiO2 composite nanofiber membrane using electrospinning for polymer electrolyte analysis, Soft Nanosci. Lett. 03 (2013) 37–43, https://doi.org/10.4236/snl.2013.32007.

[22] Z. Wang, D. Hou, S. Lin, Composite membrane with underwater-oleophobic surface for anti- oil-fouling membrane distillation, Environ. Sci. Technol. 50 (2016) 3866–3874, https://doi.org/10.1021/acs.est.5b05976.

[23] M. Zhang, S. Feng, L. Wang, Y. Zheng, Lotus effect in wetting and self-cleaning, Biotribology 5 (2016) 31–43, https://doi.org/10.1016/j.biotri.2015.08.002.

[24] P. Gould, Smart, clean surfaces, Mater. Today 6 (2003) 44–48, https://doi.org/10.1016/S1369-7021(03)01131-3.

[25] S.S. Latthe, C. Terashima, K. Nakata, A. Fujishima, Superhydrophobic surfaces developed by mimicking hierarchical surface morphology of lotus leaf, Molecules 19 (2014) 4256–4283, https://doi.org/10.3390/molecules19044256.

[26] M. Rezaei, W. Samhaber, Wetting behaviour of superhydrophobic membranes coated with nanoparticles in membrane distillation, Chem. Eng. Trans. 47 (2016) 373–378, https://doi.org/10.3303/CET1647063.

[27] X. Wu, B. Zhao, L. Wang, Z. Zhang, J. Li, X. He, H. Zhang, X. Zhao, H. Wang, Superhydrophobic PVDF membrane induced by hydrophobic SiO2 nanoparticles and its use for CO2 absorption, Sep. Purif. Technol. 190 (2018) 108–116, https://doi.org/10.1016/j.seppur.2017.07.076.

[28] Y. Chen, M. Tian, X. Li, Y. Wang, A.K. An, J. Fang, T. He, Anti-wetting behavior of negatively charged superhydrophobic PVDF membranes in direct contact membrane distillation of emulsified wastewaters, J. Memb. Sci. 535 (2017) 230–238, https://doi.org/10.1016/j.memsci.2017.04.040.

[29] N.A. Ahmad, C.P. Leo, A.L. Ahmad, W.K.W. Ramli, Membranes with great hydrophobicity: a review on preparation and characterization, Sep. Purif. Rev. 44 (2015) 109–134, https://doi.org/10.1080/15422119.2013.848816.

[30] L.D. Tijing, Y.C. Woo, J.S. Choi, S. Lee, S.H. Kim, H.K. Shon, Fouling and its control in membrane distillation-a review, J. Memb. Sci. 475 (2015) 215–244, https://doi.org/10.1016/j.memsci.2014.09.042.

[31] L.N. Nthunya, L. Gutierrez, S. Derese, B.B. Mamba, Adsorption of phenolic compounds by polyacrylonitrile nano fi bre membranes: a pretreatment for the removal of hydrophobic bearing compounds from water, J. Environ. Chem. Eng. 7 (2019) 103254, , https://doi.org/10.1016/j.jece.2019.103254.

[32] A. Alkhudhiri, N. Darwish, N. Hilal, Membrane distillation: a comprehensive review, Desalination 287 (2012) 2–18, https://doi.org/10.1016/j.desal.2011.08.027.

[33] N. Thomas, M.O. Mavukkandy, S. Loutatidou, H.A. Arafat, Membrane distillation research and implementation: lessons from the past five decades, Sep. Purif. Technol. 189 (2017) 108–127, https://doi.org/10.1016/j.seppur.2017.07.069.

[34] K.R. Zodrow, E. Bar-Zeev, M.J. Giannetto, M. Elimelech, Biofouling and microbial communities in membrane distillation and reverse osmosis, Environ. Sci. Technol. 48 (2014) 13155–13164, https://doi.org/10.1021/es503051t.

[35] J. Phattaranawik, A.G. Fane, A.C.S. Pasquier, W. Bing, A novel membrane bioreactor based on membrane distillation, Desalination 223 (2008) 386–395, https://doi.org/10.1016/j.desal.2007.02.075.

[36] M.A. Owili, Assesment of Impact of Sewage Effluents on Coastal Water Quality in Hafnarfjordur, (2003) (Accessed: September 12, 2018)., Iceland, Iceland, http://www.unuftp.is/static/fellows/document/monicaprf03.pdf.

[37] L.N. Nthunya, M.L. Masheane, S.P. Malinga, E.N. Nxumalo, T.G. Barnard, M. Kao, Z.N. Tetana, S.D. Mhlanga, Greener approach to prepare electrospun antibacterial β-cyclodextrin/Cellulose acetate nanofibers for removal of bacteria from Water, ACS Sustain. Chem. Eng. 5 (2017) 153–160, https://doi.org/10.1021/acssuschemeng.6b01089.

[38] L.N. Nthunya, M.L. Masheane, S.P. Malinga, T.G. Barnard, E.N. Nxumalo, B.B. Mamba, S.D. Mhlanga, UV-assisted reduction of in situ electrospun antibacterial chitosan-based nanofibres for removal of bacteria from water, RSC Adv. 6 (2016) 95936–95943, https://doi.org/10.1039/C6RA19472A.

[39] A.D. Frock, R.M. Kelly, Extreme thermophiles : moving beyond single-enzyme biocatalysis, Curr. Opin. Chem. Eng. 1 (2012) 363–372, https://doi.org/10.1016/j.coche.2012.07.003.

[40] J. Escorihuela, S.P. Pujari, H. Zuilhof, Organic monolayers by B(C6F5)3-catalyzed siloxanation of oxidized silicon surfaces, Langmuir 33 (2017) 2185–2193, https://doi.org/10.1021/acs.langmuir.7b00110.

[41] J. Iwasa, K. Kumazawa, K. Aoyama, H. Suzuki, S. Norimoto, T. Shimoaka, T. Hasegawa, In situ observation of a self-assembled monolayer formation of octadecyltrimethoxysilane on a silicon oxide surface using a high-speed atomic force microscope, J. Phys. Chem. C. 120 (2016) 2807–2813, https://doi.org/10.1021/acs.jpcc.5b11460.

[42] Y. Wang, M. Lieberman, Growth of ultrasmooth octadecyltrichlorosilane self-assembled monolayers on SiO2, Langmuir 19 (2003) 1159–1167, https://doi.org/10.1021/la020697x.

[43] L.N. Nthunya, L. Gutierrez, L. Lapeire, K. Verbeken, N. Zaouri, E.N. Nxumalo, B.B. Mamba, A.R. Verliefde, S.D. Mhlanga, Fouling resistant PVDF nanofibre membranes for the desalination of brackish water in membrane distillation, Sep. Purif. Technol. 228 (2019) 115793, , https://doi.org/10.1016/j.seppur.2019.115793.

[44] L.N. Nthunya, S. Derese, L. Gutrierrez, A.R. Verliefde, B.B. Mamba, T.G. Barnard, S.D. Mhlanga, Green synthesis of silver nanoparticles using one-pot and microwave-assisted methods and their subsequent embedment on PVDF nanofibre membranes for growth inhibition of mesophilic and thermophilic bacteria, New J. Chem. 43 (2019) 4168–4180, https://doi.org/10.1039/c8nj06160b.

[45] L.N. Nthunya, L. Gutierrez, R. Verliefde, S.D. Mhlanga, Enhanced flux in direct contact membrane distillation using superhydrophobic PVDF nanofibre membranes embedded with organically modified SiO2 nanoparticles, Chem. Technol. Biotechnol. 94 (2019) 2826–2837, https://doi.org/10.1002/jctb.6104.

[46] L.N. Nthunya, M.L. Masheane, S.P. Malinga, E.N. Nxumalo, S.D. Mhlanga, Environmentally benign chitosan-based nanofibres for potential use in water treatment, Cogent Chem. 3 (2017) 1–17, https://doi.org/10.1080/23312009.2017.1357865.

[47] L.N. Nthunya, M.L. Masheane, S.P. Malinga, E.N. Nxumalo, B.B. Mamba, S.D. Mhlanga, Thermally and mechanically stable cyclodextrin/cellulose acetate nanofibers synthesized using an environmentally benign procedure, Int. J. Smart Nano Mater. 8 (2017) 1–19, https://doi.org/10.1080/19475411.2017.1289276.

[48] L.N. Nthunya, L. Gutierrez, N. Khumalo, S. Derese, B.B. Mamba, A.R. Verliefde, S.D. Mhlanga, Superhydrophobic PVDF nanofibre membranes coated with an organic fouling resistant hydrophilic active layer for direct-contact membrane distillation, Colloids Surf. A Physicochem. Eng. Asp. 575 (2019) 363–372, https://doi.org/10.1016/j.colsurfa.2019.05.031.

[49] N. Khumalo, L. Nthunya, S. Derese, M. Motsa, A. Verliefde, Water recovery from hydrolysed human urine samples via direct contact membrane distillation using PVDF / PTFE membrane, Sep. Purif. Technol. 211 (2019) 610–617, https://doi.org/10.1016/j.seppur.2018.10.035.

[50] N. Khumalo, L. Nthunya, S. Derese, M. Motsa, A. Verliefde, A. Kuvarega, B.B. Mamba, S. Mhlanga, D.S. Dlamini, Water recovery from hydrolysed human urine samples via direct contact membrane distillation using PVDF/PTFE membrane, Sep. Purif. Technol. 211 (2019) 610–617, https://doi.org/10.1016/j.seppur.2018.10.035.

[51] T.O. Mahlangu, J.M. Thwala, B.B. Mamba, A. D'Haese, A.R.D. Verliefde, Factors governing combined fouling by organic and colloidal foulants in cross-flow nanofiltration, J. Memb. Sci. 491 (2015) 53–62, https://doi.org/10.1016/j.memsci.2015.03.021.

[52] L. Gutierrez, T.H. Nguyen, Interactions between rotavirus and natural organic matter isolates with different physicochemical characteristics, Langmuir 29 (2013) 14460–14468, https://doi.org/10.1021/la402893b.

[53] L. Gutierrez, C. Aubry, R. Valladares Linares, J.P. Croue, Natural organic matter interactions with polyamide and polysulfone membranes: formation of conditioning

film, Colloids Surf. A Physicochem. Eng. Asp. 477 (2015) 1–8, https://doi.org/10.1016/j.colsurfa.2015.03.031.
[54] A. Zarebska, D.R. Nieto, K.V. Christensen, B. Norddahl, Ammonia recovery from agricultural wastes by membrane distillation: fouling characterization and mechanism, Water Res. 56 (2014) 1–10, https://doi.org/10.1016/j.watres.2014.02.037.
[55] J. Sun, C. Hu, K. Zhao, M. Li, J. Qu, H. Liu, Enhanced membrane fouling mitigation by modulating cake layer porosity and hydrophilicity in an electro-coagulation/oxidation membrane reactor (ECOMR), J. Memb. Sci. 550 (2018) 72–79, https://doi.org/10.1016/j.memsci.2017.12.073.
[56] P. Kanagaraj, A. Nagendran, D. Rana, T. Matsuura, S. Neelakandan, T. Karthikkumar, A. Muthumeenal, Influence of N -phthaloyl chitosan on poly (ether imide) ultrafiltration membranes and its application in biomolecules and toxic heavy metal ion separation and their antifouling properties, Appl. Surf. Sci. 329 (2015) 165–173, https://doi.org/10.1016/j.apsusc.2014.12.082.
[57] C. Dong, Z. Wang, J. Wu, Y. Wang, J. Wang, S. Wang, A green strategy to immobilize silver nanoparticles onto reverse osmosis membrane for enhanced antibiofouling property, Desalination 401 (2017) 32–41, https://doi.org/10.1016/j.desal.2016.06.034.
[58] S. Subramanian, R. Seeram, New directions in nano fi ltration applications — are nano fi bers the right materials as membranes in desalination? Desalination 308 (2013) 198–208, https://doi.org/10.1016/j.desal.2012.08.014.
[59] T.W. Chen, S.J. Chang, G.C.C. Niu, Y.T. Hsu, S.M. Kuo, Alginate-coated chitosan membrane for guided tissue regeneration, J. Appl. Polym. Sci. 102 (2006) 4528–4534, https://doi.org/10.1002/app.24945.
[60] K.Y. Lee, D.J. Mooney, Alginate: properties and biomedical applications Kuen, Prog. Polym. Sci. 37 (2000) 106–126, https://doi.org/10.1016/j.progpolymsci.2011.06.003.Alginate.
[61] I. Barák, K. Muchová, The role of lipid domains in bacterial cell processes, Int. J. Mol. Sci. 14 (2013) 4050–4065, https://doi.org/10.3390/ijms14024050.
[62] A. Krasowska, K. Sigler, How microorganisms use hydrophobicity and what does this mean for human needs? Front. Cell. Infect. Microbiol. 4 (2014) 1–7, https://doi.org/10.3389/fcimb.2014.00112.
[63] J. Lyklema, W. Norde, G. Schraa, A.J.B. Zehnder, C.M. Mark, The role of bacterial cell wall hydrophobicity in Adhesion, Appl. Environ. Microbiol. 53 (1987) 1893–1897 doi:0099-2240/87/081893-05$02.00/0.
[64] G. Naidu, S. Jeong, S.J. Kim, I.S. Kim, S. Vigneswaran, Organic fouling behavior in direct contact membrane distillation, Desalination 347 (2014) 230–239, https://doi.org/10.1016/j.desal.2014.05.045.
[65] J. hua Li, D. bin Zhang, X. xing Ni, H. Zheng, Q. qing Zhang, Excellent hydrophilic and anti-bacterial fouling PVDF membrane based on ag nanoparticle self-assembled PCBMA polymer brush, Chinese J. Polym. Sci. (English Ed. 35 (2017) 809–822, https://doi.org/10.1007/s10118-017-1944-3.
[66] M.M. Motsa, B.B. Mamba, A.R.D. Verliefde, Forward osmosis membrane performance during simulated wastewater reclamation: fouling mechanisms and fouling layer properties, J. Water Process Eng. 23 (2018) 109–118, https://doi.org/10.1016/j.jwpe.2018.03.007.
[67] W. Qin, J. Zhang, Z. Xie, D. Ng, Y. Ye, S.R. Gray, M. Xie, Synergistic effect of combined colloidal and organic fouling in membrane distillation: measurements and mechanisms, Environ. Sci. Water Res. Technol. 3 (2017) 119–127, https://doi.org/10.1039/C6EW00156D.
[68] A. Tiraferri, Y. Kang, E.P. Giannelis, M. Elimelech, Superhydrophilic thin-film composite forward osmosis membranes for organic fouling control: fouling behavior and antifouling mechanisms, Environ. Sci. Technol. 46 (2012) 11135–11144, https://doi.org/10.1021/es3028617.
[69] J. Zhang, Z. Song, B. Li, Q. Wang, S. Wang, Fabrication and characterization of superhydrophobic poly (vinylidene fluoride) membrane for direct contact membrane distillation, Desalination 324 (2013) 1–9, https://doi.org/10.1016/j.desal.2013.05.018.
[70] Y. Huang, Z. Wang, J. Jin, S. Lin, Novel Janus membrane for membrane distillation with simultaneous fouling and wetting resistance, Environ. Sci. Technol. 51 (2017) 13304–13310, https://doi.org/10.1021/acs.est.7b02848.